

## Reduction-Oxidation and Catalytic Properties of $\text{La}_{1-x}\text{Sr}_x\text{CoO}_3$

TEIJI NAKAMURA,<sup>1</sup> MAKOTO MISONO,<sup>2</sup> AND YUKIO YONEDA

*Department of Synthetic Chemistry, Faculty of Engineering, The University of Tokyo, Bunkyo-ku, Tokyo, 113 Japan*

Received December 29, 1982; revised April 5, 1983

Catalytic oxidations of carbon monoxide, propane, and methanol have been investigated over perovskite-type mixed oxides ( $\text{La}_{1-x}\text{Sr}_x\text{CoO}_{3-\delta}$ ,  $x = 0, 0.1, 0.2, 0.4,$  and  $0.6$ ) by the use of flow and pulse methods. The reduction-oxidation properties as well as nonstoichiometry ( $\delta$ ) and desorptivity of oxygen were also measured. These properties were correlated with the catalytic activity with emphasis on the effect of the Sr substitution. Reducibility (or oxidizing ability) of these catalysts greatly increased with the extent of Sr substitution ( $x$ ), while the reoxidation became much slower with increasing  $x$ . The catalytic activities increased with  $x$  when  $x$  was low, but decreased at higher  $x$  values. This variation of activity was well explained on the basis of a redox-like mechanism, taking account of the reduction-oxidation properties of catalyst. The oxidation state of the catalysts during the steady-state catalytic oxidation of carbon monoxide varied with  $x$  and  $\text{CO}/\text{O}_2$  ratio also in accordance with the above explanation.

### INTRODUCTION

Perovskite-type mixed oxides ( $\text{ABO}_3$ ) are suitable materials for the basic study of the relationships between the solid state chemistry of metal oxides and the catalytic action, since their bulk structures have been well characterized and the oxidation state of B-site ion and the number of oxygen vacancies can be controlled by the substitution of the constituting elements without affecting the fundamental structure (1). As for the application as practical catalysts, some of the perovskite-type mixed oxides have been suggested as possible substitutes for noble metals in automotive exhaust catalysts (2). Manganite and cobaltate perovskites have been reported to be very active for the oxidation of CO (3) and the reduction of NO (4). These oxides are also active hydrogenolysis and hydrogenation catalysts (2, 5, 6).

We previously reported that  $\text{La}_{1-x}\text{Sr}_x\text{CoO}_3$  catalysts showed high activities for

the oxidation of  $\text{C}_3\text{H}_8$ ,  $\text{CH}_4$ , and  $\text{CO}$ , which varied with the  $\text{Sr}^{2+}$  content,  $x$  (7). We also found that the reducibility, the ease of oxygen desorption, the diffusivity of oxygen in the bulk, and the ability to activate the oxygen molecule markedly increased with  $x$ , and indicated that these properties are closely associated with the catalytic activities for oxidation (8).

In the present work we investigated the reduction-oxidation properties of perovskite catalysts and the reactivities of lattice and adsorbed oxygen. Emphasis has been directed toward elucidating the effects of Sr substitution on the catalytic activity as it relates to changes in the oxidation state of cobalt and the tendency to form oxygen defects.

### EXPERIMENTAL

#### *Catalysts*

The catalysts were prepared from mixtures of metal acetates in the same manner as described in the previous papers (7, 8). Powder X-ray diffraction patterns (XRD) were recorded with an X-ray diffractometer (Rigaku Denki, Rotaflex, RU-200) using

<sup>1</sup> Present address: Tonen Sekiyukagaku K. K.

<sup>2</sup> To whom all correspondence should be addressed.

CuK $\alpha$  radiation. All of the La<sub>1-x</sub>Sr<sub>x</sub>CoO<sub>3</sub> samples used in this work showed only the diffraction peaks of the perovskite-type structure.

### Apparatus

Conventional pulse, flow, and closed-circulation systems were used for the reactions. The adsorption (absorption) of oxygen was measured in a static system equipped with a Baratron pressure gauge.

### Procedure

(i) *Oxidations of C<sub>3</sub>H<sub>8</sub> and CO (flow method)*. The oxidation reactions of C<sub>3</sub>H<sub>8</sub> (at 227°C) and CO (at 150°C) were carried out with the flow system. Prior to the reaction, the catalysts (300 mg for C<sub>3</sub>H<sub>8</sub> and 50 mg for CO) were treated in an O<sub>2</sub> stream for 1 h at 300°C. The pretreatment of catalyst at 300°C for 1 h in an O<sub>2</sub> stream (1 atm) or in circulating O<sub>2</sub> (100 Torr; with a liquid nitrogen trap, for procedures (iii) and (iv)) will be called the standard pretreatment. A gas mixture of C<sub>3</sub>H<sub>8</sub> or CO (0.83%), O<sub>2</sub> (33.3%), and N<sub>2</sub> (balance) was used for flow experiments. The flow rate of the mixed gas was 60 cm<sup>3</sup>/min. Products were analyzed by a gas chromatograph (silica gel, 1 m, kept at 84°C for CO<sub>2</sub> and C<sub>3</sub>H<sub>8</sub>, and molecular sieve 5 A, 1.5 m, kept at 84°C for O<sub>2</sub>, N<sub>2</sub>, and CO).

(ii) *Oxidations of CO, CH<sub>3</sub>OH, and C<sub>3</sub>H<sub>8</sub> (pulse method)*. After the standard pretreatment (see above), the carrier gas was changed to He (the flow rate: 30 cm<sup>3</sup> min<sup>-1</sup>), and the catalysts (50 mg) were subjected to pulse reactions. The quantity of the CO and C<sub>3</sub>H<sub>8</sub> pulses was 0.1 cm<sup>3</sup> (gas) and that of CH<sub>3</sub>OH was 1  $\mu$ l (liquid). Reaction temperature was 150°C for CO and CH<sub>3</sub>OH, and 300°C for C<sub>3</sub>H<sub>8</sub>. Products were analyzed by a gas chromatograph (Porapak Q, 1.5 m, 83°C).

(iii) *Reduction and reoxidation of catalysts, and catalytic oxidation (circulation system)*. The volume of the circulation system was about 250 cm<sup>3</sup>. After the standard pretreatment, the catalysts (300 mg) were

cooled to 150°C in O<sub>2</sub>, and evacuated for 1 h at 150°C. Then the catalysts were reduced by CO at 150°C (initial CO pressure was about 15 Torr). After the reduction by about 5% (e.g., from LaCoO<sub>3</sub> to LaCoO<sub>2.85</sub>), the reduced catalysts were evacuated for 0.5 h and reoxidized by O<sub>2</sub> (initial pressure of O<sub>2</sub> was about 40 Torr). The rates of the reduction and reoxidation were measured by the pressure decrease of CO and O<sub>2</sub>, respectively, where product CO<sub>2</sub> was condensed by a trap kept at liquid nitrogen temperature. In the catalytic oxidation, the catalysts (50 mg) were diluted with SiC (250 mg) to avoid a rise in the temperature of the catalysts which might be caused by the heat of reaction.

(iv) *The degree of reduction of catalysts during the catalytic oxidation reaction (circulation system)*. After the standard pretreatment, a gas mixture ( $P_{\text{CO}} \approx 50$  Torr,  $P_{\text{O}_2} \approx 7$  Torr) was introduced onto the catalysts at 150°C. The reactions were interrupted after various reaction periods, and the reaction gas was evacuated. Then the amount of CO<sub>2</sub> formed, which was collected by a trap kept at liquid nitrogen temperature, was measured. The amount of oxygen consumption was calculated from the pressure decrease and the amount of CO<sub>2</sub> formed. The total pressure decrease after 10 min was ca. 20 Torr (see Fig. 8). In addition, to confirm the above analysis the reaction gas mixtures were also analyzed by using a quadrupole-type mass spectrometer (NEVA, NAG-531).

(v) *Adsorption (absorption) of oxygen*. First, the catalysts (1 or 0.5 g) were heated in O<sub>2</sub> (ca. 20 Torr) at 300°C for 1 h. After the system was evacuated at 300°C for 0.5 h, oxygen was introduced at 300°C. Then the temperature was lowered stepwise to 200, 100, and 25°C in the presence of O<sub>2</sub> (ca. 10 Torr). First, the amounts of oxygen uptake at each temperature were cumulatively measured. At each temperature, the amount of reversible oxygen uptake was also measured, after the sample was evacuated for 0.5 h. This oxygen will

be called reversibly ab(ad)sorbed oxygen.

(vi) *The measurement of nonstoichiometry,  $\delta$ .* The nonstoichiometry,  $\delta$ , was calculated by analyzing the amount of  $\text{Co}^{4+}$  and the total amount of Co. The total amount of Co was determined as follows (9). A sample (ca. 100 mg) was dissolved in 25 ml of 1 N  $\text{H}_2\text{SO}_4$ . After this solution was neutralized by sodium bicarbonate (5 g in excess), 5 ml of 30%  $\text{H}_2\text{O}_2$  was added. The residual  $\text{H}_2\text{O}_2$  was decomposed by gentle heating. Then the solution was diluted with water to 100 ml and 5 g of potassium iodide was added. After the solution was carefully neutralized by HCl (10 ml in excess), it was titrated with a standard thiosulfate solution (N/50).

The determination of the amount of  $\text{Co}^{4+}$  and  $\text{Co}^{3+}$  was carried out according to the literature (10). The sample (about 100 mg) was dissolved in the solution of 25 ml of 0.4 N HCl plus 25 ml of 0.16 M KI. The solution was titrated with a standard thiosulfate solution.

## RESULTS

### *Nonstoichiometry of $\text{La}_{1-x}\text{Sr}_x\text{CoO}_{3-\delta}$*

The values of  $\delta$  in  $\text{La}_{1-x}\text{Sr}_x\text{CoO}_{3-\delta}$  ( $x = 0 - 0.6$ ), which had been calcined at 850°C, cooled in air, treated in oxygen at 300°C, and then cooled in oxygen to room temperature, were determined as summarized in Table 1. The  $\delta$  value increased with the  $\text{Sr}^{2+}$  content,  $x$ . Figure 1 shows the results of  $\text{O}_2$  adsorption (absorption) for these samples. The open symbols express the cumulative amounts of oxygen which were adsorbed when the samples were cooled stepwise after  $\text{O}_2$  was introduced at 300°C. Differences between open and closed symbols are the amounts of reversible ad(ab)sorption at each temperature. These amounts are of comparable order with those obtained by the temperature programmed desorption (TPD) of oxygen as previously reported (8). The values of  $\delta$  in vacuum ( $10^{-3}$  Torr) and in  $\text{O}_2$  (ca. 20 Torr) at 300°C are given in Table 1, where  $\Delta\delta$  which was calculated

TABLE I

 The Nonstoichiometry ( $\delta$ ) of  $\text{La}_{1-x}\text{Sr}_x\text{CoO}_{3-\delta}$ <sup>a</sup>

$x$	$\left[\frac{\text{Co}^{4+}}{\text{Co}^{3+} + \text{Co}^{4+}}\right]^b$	$\delta^b$	$\Delta\delta^c$	
			Under vacuum	In $\text{O}_2$ (~10 Torr)
0	(0)	(0)	0.0011	0.00046
0.2	$0.20 \pm 0.01$	$\pm 0.005$	0.0049	0.0012
0.4	0.30	0.052	0.036	0.012
0.6	0.40	0.098	0.060	0.014

<sup>a</sup> Calcined at 850°C. Surface areas are 2.5 ( $x = 0$ ), 4.3 ( $x = 0.2$ ), 5.4 ( $x = 0.4$ ), and 3.5  $\text{m}^2/\text{g}$  ( $x = 0.6$ ).

<sup>b</sup> Chemical analysis (see text). Samples were pretreated in  $\text{O}_2$  at 300°C and cooled to room temperature.

<sup>c</sup> [ $\delta$  value at 300°C] - [ $\delta$  value at room temperature]. Calculated from the amount of  $\text{O}_2$  uptake.

from the amount of  $\text{O}_2$  uptake represents the difference between the  $\delta$  values and the  $\delta$  value at room temperature. The values of  $\delta$  and  $\Delta\delta$  both increased with  $x$ .

Figure 2 shows the uptake of oxygen after the catalysts were evacuated at 300 or 400°C. The initial rate for  $x = 0.4$  was greater than that for  $x = 0.6$ . When the initial pressure of oxygen was changed, the rate was positively dependent on the oxygen pressure (about 0.4th order) for the catalyst with  $x = 0.6$ , as in the case of reoxida-

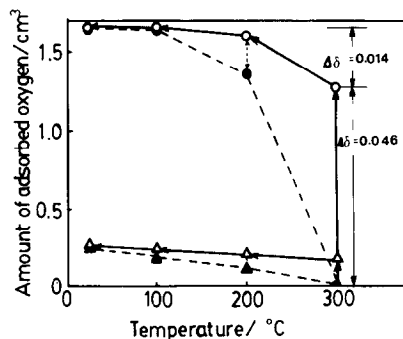


FIG. 1. The amounts of  $\text{O}_2$  adsorption/absorption. Catalyst weight: 500 mg for  $x = 0.6$  and 1.0 g for  $x = 0.2$ . Circles and triangles refer to  $x = 0.6$  and 0.2, respectively. Open symbols represent the amount of  $\text{O}_2$  uptake at each temperature in  $\text{O}_2$  (20 Torr) after the samples were evacuated at 300°C. Closed symbols were the amounts after evacuation at each temperature.  $\Delta\delta$ 's are  $\text{O}_2$  uptake expressed by the differences in  $\delta$  in  $\text{La}_{0.4}\text{Sr}_{0.6}\text{CoO}_{3-\delta}$ .

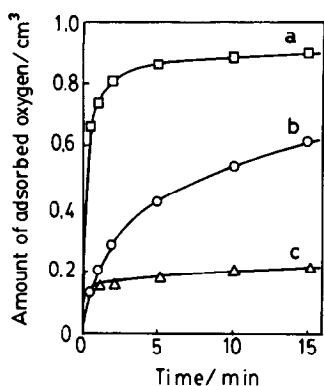


FIG. 2. O<sub>2</sub> uptake at 150°C. Catalyst weight: 500 mg for  $x = 0.4$  and  $0.6$ , 1.0 g for  $x = 0.2$ . (a)  $x = 0.4$  (preevacuated at 300°C). (b)  $x = 0.6$  (preevacuated at 300°C). (c)  $x = 0.2$  (preevacuated at 400°C). The uptake of this sample evacuated at 300°C was very small (see Fig. 1).

tion (see below). The adsorption isotherms exhibited saturation at about 10 Torr for LaCoO<sub>3</sub> and La<sub>0.8</sub>Sr<sub>0.2</sub>CoO<sub>3</sub> at 300°C.

#### Oxidation Reaction (Flow Method)

Figure 3 shows the results of the catalytic oxidation reaction of C<sub>3</sub>H<sub>8</sub> and CO. In both cases, the rate increased with  $x$  up to La<sub>0.8</sub>Sr<sub>0.2</sub>CoO<sub>3</sub> and became nearly constant or decreased slightly with further increase in  $x$ .

#### Oxidation Power (or Reducibility) of La<sub>1-x</sub>Sr<sub>x</sub>CoO<sub>3</sub>

Figures 4 and 5 show the results of pulse reactions of CH<sub>3</sub>OH, CO, and C<sub>3</sub>H<sub>8</sub>. Only CO<sub>2</sub> and H<sub>2</sub>O were formed from CH<sub>3</sub>OH

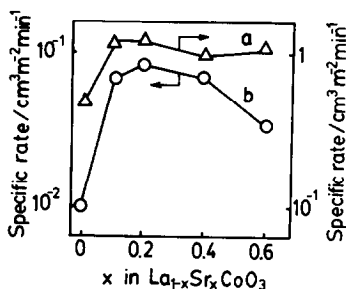


FIG. 3. Effects of the Sr substitution for La in the catalytic oxidation (flow method). (a) Oxidation of CO at 150°C. (b) Oxidation of C<sub>3</sub>H<sub>8</sub> at 227°C.

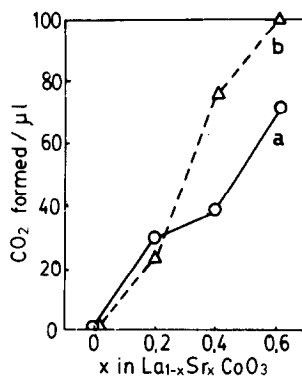


FIG. 4. Amounts of CO<sub>2</sub> formed from the pulses of CO or CH<sub>3</sub>OH plotted as a function of  $x$ . Catalyst weight: 50 mg, reaction temperature: 150°C. Pulse size: CO, 1 cm<sup>3</sup>; CH<sub>3</sub>OH, 1 μl. (a) CH<sub>3</sub>OH, (b) CO.

and C<sub>3</sub>H<sub>8</sub>. When these reactants were pulsed in the absence of oxygen, the extent of CO<sub>2</sub> formation, which reflects the oxidation power of catalyst, increased with  $x$  in the three cases. On the other hand, when C<sub>3</sub>H<sub>8</sub> was copulsed with O<sub>2</sub>, the amounts of CO<sub>2</sub> formed increased with  $x$  up to  $x = 0.2$  but decreased for  $x \geq 0.4$ . The latter trend closely resembles that of catalytic activity measured in a flow system (Fig. 3).

#### Reduction and Reoxidation of the Catalyst (Circulation System)

Figure 6a shows the CO consumption in the reduction of the catalysts by CO, where

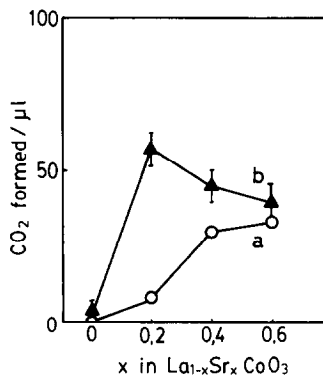


FIG. 5. Amounts of CO<sub>2</sub> formed from C<sub>3</sub>H<sub>8</sub> pulses. Catalyst weight: 50 mg, reaction temperature: 300°C. (a) C<sub>3</sub>H<sub>8</sub> only, (b) C<sub>3</sub>H<sub>8</sub> + O<sub>2</sub>. Bars indicate the range of variation when the O<sub>2</sub>/C<sub>3</sub>H<sub>8</sub> ratio was changed from 0.5 to 2.0.

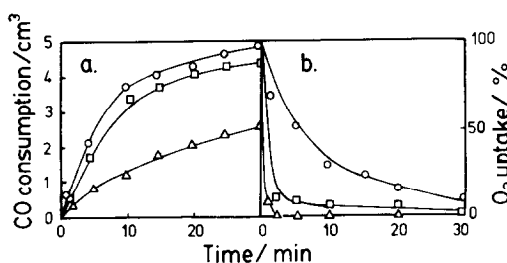


FIG. 6. Reduction by CO (a) and reoxidation by  $\text{O}_2$  (b) in a circulation system. Catalyst weight: 300 mg, reaction temperature:  $150^\circ\text{C}$ . ( $\Delta$ )  $x = 0.2$ , ( $\square$ )  $x = 0.4$ , ( $\circ$ )  $x = 0.6$ .  $\text{O}_2$  uptakes are expressed by  $[\text{CO consumption}] \times \frac{1}{2} \times 100$ .

from the slopes of the curves the initial rates of reduction are observed to increase with increasing  $x$ . The rate of reduction calculated from the slopes of the curves in Fig. 6a are plotted in Fig. 7, as a function of the degree of reduction ( $\delta'$ : difference between the  $\delta$  value after the reduction and the  $\delta$  value after the evacuation at  $150^\circ\text{C}$ ). The general trends do not change when the rates are plotted against  $\delta$  instead of  $\delta'$ , since the changes in  $\delta$  value caused by  $150^\circ\text{C}$  evacuation were small (see Fig. 1). Disproportionation of CO was not detected as described

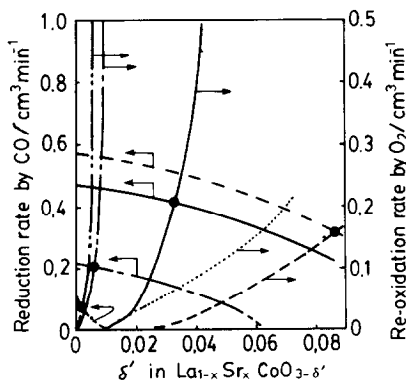


FIG. 7. Rates of reduction by CO and reoxidation by  $\text{O}_2$  as a function of  $\delta'$ . Catalyst weight: 300 mg, reaction temperature:  $150^\circ\text{C}$ . (— · — · —):  $x = 0$ , (— · —):  $x = 0.2$ , (—):  $x = 0.4$ , (— · —):  $x = 0.6$ , (· · ·):  $x = 0.6$  (2% prerduced). Reoxidation was carried out after the sample was prerduced by 5%, except for the dotted line (2%). (●) Expresses the crosspoints of the reduction and reoxidation curves.  $\delta'$ :  $\delta$  values under the assumption that  $\delta$  is zero before the reduction experiments. See text.

below. The rate of reduction for  $\text{LaCoO}_3$  decreased rapidly, and the rates of the other samples decreased slowly with the degree of reduction. The reoxidation of the catalysts which had been reduced by 5% proceeded as shown in Fig. 6b. From these data the rates of reoxidation were calculated and plotted against  $\delta'$  in Fig. 7. The rates increased rapidly with the degree of reduction, and decreased with  $x$ , when they are compared at the same degree of reduction, as preliminarily reported before (11).

The rate of reoxidation for 2% reduced  $\text{La}_{0.4}\text{Sr}_{0.6}\text{CoO}_3$  is shown by a dotted line in Fig. 7. This rate was greater than that of the 5% reduced sample at the same degree of reduction, but the difference was small as compared with the dependency of the rate on  $\delta'$ . The rate of reoxidation was 0.4–0.7th order with respect to oxygen pressure ( $P_{\text{O}_2} = 15\text{--}90$  Torr) for  $x = 0.6$  (prerduced by 5%) at  $150^\circ\text{C}$ . The carbon balance was satisfactory in the process of reduction, indicating that the formation of carbide or carbon deposit was negligible.

#### Comparison of the Catalytic Oxidation of CO and the Stoichiometric Reduction of the Catalysts by CO

In Table 2, the rates of the catalytic oxidation of CO in a circulating system are compared with the rates of the stoichiometric reduction of the catalysts by CO under similar conditions. The rate of stoichiometric reduction increased with  $x$  in a similar manner as in Figs. 4–6, and the rate for  $\text{La}_{0.4}\text{Sr}_{0.6}\text{CoO}_3$  was 50 times greater than

TABLE 2

Rates of  $\text{CO}_2$  Formation with and without  $\text{O}_2$  at  $150^\circ\text{C}$

$\text{La}_{1-x}\text{Sr}_x\text{CoO}_3$	Rate ( $\text{ml g}^{-1} \text{min}^{-1}$ )		With $\text{O}_2$ Without $\text{O}_2$
	without $\text{O}_2$	with $\text{O}_2$	
$x = 0$	0.15	1.7 ~ 1.8	11.3 ~ 12.0
$x = 0.2$	2.6	16.2 ~ 19.8	6.2 ~ 7.6
$x = 0.6$	7.6	10.4 ~ 17.0	1.4 ~ 2.2

Note. Circulation method. Initial pressure:  $p_{\text{CO}} = 15$  Torr,  $p_{\text{O}_2} = 40$  Torr.

that for  $\text{LaCoO}_3$ . On the other hand, the rate of catalytic oxidation showed a maximum at  $x = 0.2$ . The ratio of the rate of catalytic oxidation to that of stoichiometric reduction was 1.4–2.2 for  $\text{La}_{0.4}\text{Sr}_{0.6}\text{CoO}_3$ . The ratio increased with decreasing  $x$  and was about 12 for  $\text{LaCoO}_3$ .

#### The Oxidation State of Catalysts During Catalytic Oxidation of CO

The oxidation state of catalysts ( $\text{La}_{0.8}\text{Sr}_{0.2}\text{CoO}_3$ ) during the catalytic oxidation of CO can be estimated from the results shown in Fig. 8a, where open circles show the total amount of  $\text{CO}_2$  formed and triangles the amount of  $\text{CO}_2$  accounted for by the reaction of gaseous oxygen. The differences between these two values (circles and triangles) are the amount of  $\text{CO}_2$  formed from lattice oxygen, and is therefore proportional to the degree of reduction, i.e., the oxidation state (solid circles). Figure 8a shows that the catalyst was immediately reduced and reached nearly a stationary oxidation state at the initial stage of the reaction. Small variation of the oxidation state is due to the change in the  $\text{CO}/\text{O}_2$  ratio of the reaction gas.

Similar experiments were conducted for catalysts with  $x = 0$  and  $x = 0.6$ . The results summarized in Table 3 indicate that the catalyst was in a lower oxidation state (or greater degree of reduction) as  $x$  increased. When oxygen was in excess ( $P_{\text{CO}} = 16$  Torr,  $P_{\text{O}_2} = 40$  Torr) the degree of reduction naturally became smaller, but it also increased with  $x$ .

#### DISCUSSION

##### Nonstoichiometry and Structural Changes with Redox Cycle

When  $\text{Sr}^{2+}$  is partially substituted for  $\text{La}^{3+}$ , the charge is compensated by the oxidation of  $\text{Co}^{3+}$  to  $\text{Co}^{4+}$  and/or formation of oxygen vacancies, as is formulated by  $\text{La}_{1-x}^{3+}\text{Sr}_x^{2+}\text{Co}_{1-x+2\delta}^{3+}\text{Co}_{x-2\delta}^{4+}\text{O}_{3-\delta}$ . Although  $\text{Co}^{4+}$  is an ion of abnormal valence, it has

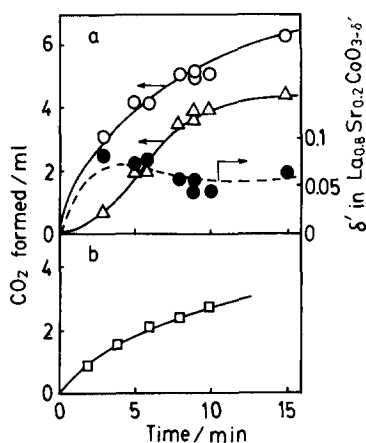


FIG. 8. Rate of catalytic oxidation of CO and reduction of catalyst by CO. Catalyst:  $\text{La}_{0.8}\text{Sr}_{0.2}\text{CoO}_3$  (300 mg), reaction temperature:  $150^\circ\text{C}$ . (a) Catalytic oxidation (CO: 50 Torr,  $\text{O}_2$ : 7 Torr). (○) Total amounts of  $\text{CO}_2$  formed. (△) Amounts of  $\text{CO}_2$  formed by the reaction between CO and gaseous  $\text{O}_2$ . (●) Degrees of reduction (differences between ○ and △). (b) Reduction of catalyst (CO: 50 Torr in the absence of  $\text{O}_2$ ). (□) Amounts of  $\text{CO}_2$  formed.

been observed in  $\text{BaCoO}_3$  (9),  $\text{SrCoO}_{3-\delta}$  (12), and  $\text{La}_{1-x}\text{Sr}_x\text{CoO}_{3-\delta}$  (13). For the samples used in the present investigation (Table 1),  $\text{Co}^{4+}$  was formed without creating oxygen vacancies for  $x = 0.2$ , but the oxygen vacancies were formed for  $x = 0.4$  and  $0.6$ . For example, 40% of the Co in  $\text{La}_{0.4}\text{Sr}_{0.6}\text{CoO}_3$  was  $\text{Co}^{4+}$ , and  $\delta$  was about 0.1. These results agree with the results of Jonker and Van Santen (13) that  $\text{Co}^{4+}$  was formed without the formation of oxygen vacancies for  $x$

TABLE 3

Degree of reduction of  $\text{La}_{1-x}\text{Sr}_x\text{CoO}_3$  during CO oxidation at  $150^\circ\text{C}$

Initial pressure (Torr)	$P_{\text{O}_2}$	$\delta'$ in $\text{La}_{1-x}\text{Sr}_x\text{CoO}_{3-\delta}$		
		$x = 0$	$x = 0.2$	$x = 0.6$
50	7	0.007	0.06	0.12
15	40	0	0.004	0.017

Reaction time; 4–6 min.

$\delta'$  is the change in the nonstoichiometry referred to that after the  $150^\circ\text{C}$  evacuation (see text).

$\leq 0.4$ , but that oxygen vacancies were formed in addition to  $\text{Co}^{4+}$  when  $x$  exceeded 0.4. Therefore, the  $\delta$  value of  $\text{LaCoO}_3$  in this study may be suspected to be zero, although the chemical analysis was not carried out. Consequently, the compositions of the samples after the standard treatment in the present investigation are close to  $\text{LaCoO}_3$ ,  $\text{La}_{0.8}\text{Sr}_{0.2}\text{CoO}_3$ ,  $\text{La}_{0.6}\text{Sr}_{0.4}\text{CoO}_{2.95}$ , and  $\text{La}_{0.4}\text{Sr}_{0.6}\text{CoO}_{2.90}$ .

According to Crespin and Hall (6),  $\text{LaCoO}_3$  reduced by 3 electrons/mol was partially decomposed to form  $\text{La}_2\text{O}_3$  and  $\text{Co}^\circ$ , although  $\text{Co}^\circ$  was not detected by XRD. Even in this case, the structure of perovskite was completely restored by the reoxidation. These results indicate that the perovskite structure is decomposed when it is extensively reduced, but the structure can be restored by reoxidation in some cases.

Therefore, the restoration of the perovskite structure by reoxidation as in the present work does not automatically mean that the structure was unchanged in the reduced state. However, in the present work the extent of reduction was very small (0.3 electrons/mol as compared with 1–3 electrons/mol in the report of Crespin and Hall (6)). Moreover, the reoxidation proceeded much more easily (Fig. 2), and no XRD diffraction lines of  $\text{La}_2\text{CoO}_4$ ,  $\text{La}_4\text{Co}_3\text{O}_{10}$ ,  $\text{La}_2\text{O}_3$ ,  $\text{CoO}$ , and  $\text{Co}_3\text{O}_4$ , which were reported in the literature for the decomposition of  $\text{LaCoO}_3$  (14) were detected in the present work after reduction. Lombardo *et al.* (15) have recently reported that reduced  $\text{LaCoO}_3$  was active for the hydrogenation of ethylene since active  $\text{Co}^\circ$  particles were formed on the surface by reduction. According to their results, the activity due to  $\text{Co}^\circ$  started to appear at the reduction level of 1.5 electrons/mol. This reduction level is much greater than that in the present work. Consequently, it is presumed that the fundamental structure of perovskite is preserved during the redox cycles as long as the extent of reduction is low as in the present work.

### *Reduction and Reoxidation of the Catalysts*

First we shall discuss briefly whether the rate-determining step of the redox cycle is the surface reaction (case 1) or the diffusion of oxygen in the bulk (case 2). If the diffusion of oxygen in the bulk is very rapid and the surface reaction is rate determining (case 1), there will be no gradient of the concentration of oxygen vacancy in the bulk, and therefore the curve of the reoxidation rate as in Fig. 7 should not depend on the extent of prereduction. In other words, the rate at the same extent of reduction should be identical. But the curves for the 2 and 5% reduced samples ( $\text{La}_{0.4}\text{Sr}_{0.6}\text{CoO}_{3-\delta}$ ) were different (Fig. 7, dotted and broken lines), indicating that the diffusion is not very rapid. Our previous observation that the isotopic equilibration of oxygen in the gas phase was much more rapid than the exchange of oxygen with the bulk oxygen (8) also does not favor the assumption of rapid diffusion of oxygen. In case 2 where the diffusion determines the redox rate, the pressure dependence of reoxidation would be negative order in oxygen pressure (16), since the number of anion defects which controls the diffusion rate should decrease with the oxygen pressure. [A possible mechanism is  $\frac{1}{2}\text{O}_2 + 2\text{Co}\overset{\times}{\text{Co}} + \text{V}\overset{\circ}{\text{O}} \rightleftharpoons \text{O}\overset{\times}{\text{O}} + 2\text{Co}\overset{\circ}{\text{Co}}$ , where  $\text{Co}\overset{\times}{\text{Co}}$  and  $\text{O}\overset{\circ}{\text{O}}$  are  $\text{Co}^{3+}$  and  $\text{O}^{2-}$  at the ordinary lattice site, respectively.  $\text{V}\overset{\circ}{\text{O}}$  and  $\text{Co}\overset{\circ}{\text{Co}}$  are oxygen vacancy and  $\text{Co}^{4+}$ , respectively.] However, it was actually positive (about 0.5th order). Further, the fact that the reoxidation became slower with increase in  $x$  cannot be explained by case 2, since the rate of oxygen diffusion in the bulk should increase with the concentration of anion defects and therefore with  $x$ . Consequently, either step cannot be rate determining. A possible explanation may be that the redox cycle is a combined process of the surface reaction and the diffusion of oxygen in the bulk.

The reducibility and the readiness of oxygen desorption increased with the  $\text{Sr}^{2+}$  con-

tent,  $x$ , as shown in Figs. 4–7. Temperature-programmed desorption (TPD) of oxygen showed the same trend (8, 11). In contrast, the reoxidation became slower with increasing  $x$ , as shown in Figs. 6 and 7. There might be a possibility that the reoxidation process was influenced by the deposition of metallic cobalt or a considerable change of the structure brought about by the prereduction. However, as discussed above, the essential structure of the catalysts was not likely changed by reduction in the present work. Furthermore, as shown in Fig. 2, a similar trend in the adsorption of oxygen (reoxidation) was found for the samples which had been slightly reduced only by evacuation ( $\delta < 0.016$ ), where no structural changes were probable.

Consequently, the slower reoxidation with samples having greater  $x$  is likely due to their higher equilibrium pressure of oxygen as discussed previously (8). The reason why the effect of  $\text{Sr}^{2+}$  substitution was less significant in the case of 1200°C calcined samples (7) than in the case of 850°C calcined ones is not clear at present. Due to the very low surface area and difficulty in high-temperature control, the data for 1200°C calcination were not very reproducible.

#### *Reaction Mechanism and Active Oxygen Species*

In a redox mechanism, lattice oxygen is responsible for the catalytic oxidation, and the reaction proceeds by the repetition of reduction and reoxidation cycle of catalyst. To the first approximation, when the reaction proceeds by a redox mechanism, the rate at the crosspoint of the curves for reduction and reoxidation of each catalyst in Fig. 7 should be equal to the rate of catalytic oxidation at the steady state. The rate at the crosspoints in Fig. 7 initially increased with  $x$  and became nearly constant or slightly decreased at higher  $x$ . This trend is in general agreement with that found for the rate of catalytic oxidation (Fig. 3). Fig-

ure 7 also predicts that the extent of reduction of the catalyst at the steady state (the value of the abscissa at the crosspoint) increases with  $x$ . This trend was also experimentally confirmed as shown in Table 3.

However, the agreement was not satisfactory when examined more quantitatively. Although there was only a small difference between the rates of catalytic reactions and those of stoichiometric reactions in the case of  $\text{La}_{0.4}\text{Sr}_{0.6}\text{CoO}_3$  (Table 2), indicating that the catalytic oxidation proceeded by the redox mechanism, the catalytic oxidation became significantly more rapid than the stoichiometric reduction for  $\text{LaCoO}_3$  and  $\text{La}_{0.8}\text{Sr}_{0.2}\text{CoO}_3$ . The differences do not seem to be explained only by the differences in the oxidation state of the catalysts or in the partial pressure of CO and  $\text{O}_2$ . A possible explanation for the differences is that the adsorbed oxygen takes part under these conditions over the latter two catalysts.

Two types of catalytic processes have already been proposed for perovskite-type catalysts by Voorhoeve (1, 17); intrafacial and suprafacial catalysis. Suprafacial reactions are those for which the reaction between adsorbed species on the surface is much faster than reactions involving lattice oxygen. They are often low-temperature processes. On the other hand, intrafacial reactions are those in which the removal of oxygen from the lattice or the reverse process, that is, reduction–oxidation of the catalyst, is an important process. Tascón *et al.* (17) proposed a mechanism for the oxidation of CO over  $\text{LaCoO}_3$ , where dissociatively adsorbed oxygen reacts with adsorbed CO.

Therefore, a mechanism involving adsorbed oxygen is probable. However, we previously observed that the shape of the TPD curves are more or less similar among the catalysts ( $x = 0$ –0.6) and continuous in the temperature range of 100–600°C (8). This fact indicates that the discrimination between the adsorbed and lattice oxygen is very difficult, although oxygen desorbed at



higher temperatures in TPD is obviously lattice oxygen. Therefore, although the oxygen desorbed at low temperatures might be adsorbed oxygen, it closely reflects the reducibility of the bulk lattice oxygen, so that it could be regarded in a sense as "lattice oxygen" (11). In accordance with this idea, the oxidation state of catalysts varied depending on the reaction conditions (Table 3), and the changes with  $x$  both in the catalytic activity and in the oxidation state of catalyst at stationary state, are also explained, in general, by the redox mechanism. Even in the case of  $\text{La}_{0.8}\text{Sr}_{0.2}\text{CoO}_3$ , the rate of catalytic oxidation was close to that of stoichiometric reduction when CO was present in excess (CO: 50 Torr and  $\text{O}_2$ : 7 Torr, Figs. 8a and b).

Consequently, in the above sense the redox mechanism may be applied to all of these catalysts in the oxidation of CO. It is probable that the oxidations of  $\text{C}_3\text{H}_8$  and  $\text{CH}_4$  also proceed by redox mechanism, because similar trends in catalytic activity were observed upon Sr substitution. The active oxygen species can be supplied from both gaseous and bulk oxygen onto the surface. In the case of  $\text{LaCoO}_3$  and  $\text{La}_{0.8}\text{Sr}_{0.2}\text{CoO}_3$ , the supply from gaseous oxygen is probably faster than that from the bulk, so that the surface is, on the average, in a higher oxidation state and becomes more reactive in the presence of gaseous oxygen than in its absence. Recently, Yamazoe *et al.* (18) reported XPS data of  $\text{La}_{1-x}\text{Sr}_x\text{CoO}_3$ , in addition to TPD results which are similar to ours reported previously (8, 11). Reac-

tivity of these oxide species and their catalytic properties are an interesting subject for future study.

#### REFERENCES

1. Voorhoeve, R. J. H., "Advanced Materials in Catalysis," p. 129. Academic Press, New York, 1977.
2. Libby, W. F., *Science* **171**, 499 (1971).
3. Voorhoeve, R. J. H., Remeika, J. P., Freeland, P. E., and Mattias, B. T., *Science* **177**, 353 (1972).
4. Voorhoeve, R. J. H., Remeika, J. P., and Trimble, L. E., "The Catalytic Chemistry of Nitrogen Oxides," p. 215. Plenum, New York, 1975.
5. Ichimura, K., Inoue, Y., and Yasumori, I., *Bull. Chem. Soc. Jpn.* **54**, 1787 (1981).
6. Crespin, M., and Hall, W. K., *J. Catal.* **69**, 359 (1981).
7. Nakamura, T., Misono, M., Uchijima, T., and Yoneda, Y., *Nippon Kagaku Kaishi* **1980**, 1679.
8. Nakamura, T., Misono, M., and Yoneda, Y., *Bull. Chem. Soc. Jpn.* **55**, 394 (1982).
9. Gushee, B. E., Katz, L., and Ward, R., *J. Am. Chem. Soc.* **79**, 5601 (1957).
10. Laitinen, H. A., and Burdett, L. W., *Anal. Chem.* **23**, 1268 (1951).
11. Nakamura, T., Misono, M., and Yoneda, Y., *Chem. Lett.* **1981**, 1589.
12. Taguchi, H., Shimada, M., and Koizumi, M., *J. Solid State Chem.* **29**, 221 (1979).
13. Jonker, G. H., and Van Santen, J. H., *Physica* **19**, 120 (1953).
14. Janecek, J. J., and Wirtz, G. P., *J. Am. Ceram. Soc.* **61**, 242 (1978).
15. Petunchi, J. O., Nicastro, M. A., and Lombardo, E. A., *J. Catal.* **70**, 356 (1981).
16. Kroger, F. A., "The Chemistry of Imperfect Crystals." North-Holland, Amsterdam, 1974.
17. Tascón, J. M. D., García Fierro, J. L., and González Tejuca, L., *Z. Phys. Chem. Neue Folge* **124**, 249 (1981).
18. Yamazoe, N., Teraoka, Y., and Seiyama, T., *Chem. Lett.* **1981**, 1767.